J Porous Mater (2016) 23:1547–1556
DOI 10.1007/s10934-016-0215-y

Comparative studies on the physical properties of TEOS, TMOS and Na_2SiO_3 based silica aerogels by ambient pressure drying method

Abhijit A. Pisal[1] · **A. Venkateswara Rao**[1]

Published online: 4 June 2016

Abstract In order to compare the various precursors of silica aerogels, three different precursors namely TMOS, TEOS and Na_2SiO_3 were studied in this paper. The property differences of the aerogels caused by the three precursors were discussed in terms of reaction process, gelation time, pore size distributions, thermal conductivity, SEM, hydrophobicity and thermal stability. It has been found that the gelation time of the silica gel is strongly dependent on the type of precursor used. During the surface modification process, organic groups were attached to the wet gel skeletons transforming the hydrophilic to the hydrophobic which were characterized by Fourier Transform Infrared spectroscopy (FTIR). It has been found that the contact angle of the Na_2SiO_3 and TMOS precursor based aerogels with water have the higher contact angle of 149° and whereas Na_2SiO_3 precursor based aerogel has the lower contact angle of 130°. The thermal conductivities of the Na_2SiO_3 and TMOS based aerogels have been found to be lower (0.025 and 0.030 W m^{-1} K^{-1}, respectively) compared to the TEOS based (0.050 W m^{-1} K^{-1}) aerogels. The pore sizes obtained from the N_2 adsorption measurements varied from 40 to 180, 70 to 190, and 90 to 200 nm for the TEOS, TMOS and Na_2SiO_3 precursor based aerogels, respectively. The scanning electron microscopy studies of the aerogels indicated that the Na_2SiO_3 and TMOS based aerogels show narrow and uniform pores while the particles of SiO_2 network are very small. On the other hand, TEOS aerogel show non-uniform pores such that the numbers of smaller size pores are less compared to the pores of larger size while the SiO_2 particles of the network are larger as compared to both Na_2SiO_3 and TMOS aerogels. Hence, the surface are of the aerogels prepared using TEOS precursor has been found to be the lowest (~620 m^2 g^{-1}) compared to the Na_2SiO_3 (~868 m^2 g^{-1}) and TMOS (~764 m^2 g^{-1}) aerogels.

Keywords Silica aerogels · Hydrophobicity · Thermal conductivity · Pore size distribution · Silylation

1 Introduction

Silica aerogels consist of more than 98 % air and <2 % solid silica in the form of highly cross-linked network structure. They are unique nano-porous, low density materials having high optical transmission in the visible light, very low thermal conductivity (~0.01 W m^{-1} K^{-1}) very low sound velocity (100 m/s) and surface area as large as 1600 m^2 g [1–3]. Due to these interesting properties, silica aerogels have several technological applications such as for efficient super thermal insulating systems [4, 5] in oil spill cleanup [6] and drug delivery [7], liquid rocket propellants [8] and catalyst supports [9]. Generally, silica aerogels are prepared by hydrolysis and polycondensation of alkoxides in the presence of acid or base catalyst followed by supercritical drying. However, the supercritical alcohol drying process is expensive because an autoclave is needed and it incurs a high risk if the drying is executed on an alcohol solution [10]. Therefore, the production of low density, low thermal conductive silica aerogels on a large scale at reasonable cost still has remained a great challenge. A large number of research reports is available in the literature on the preparation of silica aerogels at ambient pressure using a surface modification prior to the drying

✉ A. Venkateswara Rao
avrao2012@gmail.com

[1] Air Glass Laboratory, Department of Physics, Shivaji University, Kolhapur, Maharashtra 416004, India

[11–13]. The physical properties like density, porosity, hydrophobicity and thermal conductivity of silica aerogels are strongly depends on the type of precursor.

The precursors used in the sol–gel process are mainly silicon alkoxides. Many of these silicon derivatives are used to synthesize silica aerogels. Each of these silicon derivative produces varying degrees of physical, thermal and mechanical properties in the silica aerogels. Some of these precursors used are Tetramethoxysilane (TMOS), tetraethoxysilane (TEOS) and water–glass (sodium silicate) [14–16]. Even though most of the published reports on silica aerogels deal with TMOS precursor [17]., TEOS precursor [18] and Na_2SiO_3 precursor [19], there is a little information in the literature regarding the comparison of physical properties like density, surface area, porosity, contact angle and thermal conductivity of silica aerogel synthesized by different precursors. Therefore, we have taken up systematic and detailed studies, and we present and discuss our results on the effect of various precursors such as TMOS, TEOS, and Na_2SiO_3 on the physical properties of silica aerogels.

2 Experimental procedures

2.1 Experimental materials

The chemicals used were: Tetramethoxysilane (TMOS), Tetraethoxysilane (TEOS) with purity of 98 %, ammonium hydroxide (from Fluka Company, Switzerland), sodium silicate solution (Na_2SiO_3, LOBA, India, Na_2SiO_3 content 36 wt%, $Na_2O{:}SiO_2 = 1{:}3.33$) of specific gravity 1.05 diluted from 1.36 specific gravity as a precursor, NH_4OH [1 M 0.1 mL] as a catalyst, oxalic acid (0.001 M $C_2H_2O_4$), Acetic acid (CH_3COOH), trimethylchlorosilane (TMCS) [Fluka, Pursis grade, Switzerland] as silylating agent, methanol (MeOH, CH_3OH) and hexane (C_6H_{14}) [Merck, India] as solvents. Triple distilled water made in silica glass containers was used throughout the experiments.

2.2 Sample preparation

Silica hydrogels were prepared by single step sol–gel process by hydrolysis and polycondensation of Na_2SiO_3 precursor in the presence of an acid catalyst as per the following chemical reactions:

$$\underset{\text{SodiumSilicate}}{Na_2SiO_3} + H_2O + \underset{\text{Aceticacid}}{2CH_3COOH} \rightarrow \underset{\text{Silicicacid}}{Si(OH)_4} + \underset{\text{Sodiumacetate}}{2CH_3COONa} \quad (1)$$

$$\underset{\text{Silicicacid}}{Si(OH)_4} + (HO)_4Si \rightarrow (HO)_3 - \underset{\text{Silicasurface}}{Si - O - Si} - (OH)_3 + \underset{\text{Water}}{H_2O} \quad (2)$$

While, the silica alcogels based on TEOS and TMOS precursors (silicon alkoxides) were prepared by hydrolysis and polycondensation of solvent (alcohol) diluted alkoxide in the presence of a catalyst. The hydrolysis and polycondensation reaction mechanism for tetraethoxysilane (TEOS) precursor is as given below.

2.2.1 Hydrolysis

$$\underset{\text{Tetraethylorthosilicate}}{Si(OC_2H_5)_4} + 4H_2O \longrightarrow \underset{\text{Silicic acid}}{Si(OH_4)} + 4\underset{\text{Ethanol}}{C_2H_5OH} \quad (3)$$

2.2.2 Condensation

$$\underset{\text{Silicicacid}}{Si(OH_4)} + Si(OH_4) \rightarrow = Si - O - Si = + \underset{\text{Water}}{4H_2O} \quad (4)$$

$$\underset{\text{Silicicacid}}{Si(OH_4)} + \underset{\text{Tetraethylorthosilicate}}{Si(OC_2H_5)_4} \rightarrow = \underset{\text{Silicasurface}}{Si - O - Si} = + \underset{\text{Ethanol}}{4C_2H_5OH} \quad (5)$$

Similarly, tetramethoxysilane (TMOS) follow the same trend of chemical reactions.

The preparation plan for the synthesis of silica aerogels by ambient pressure drying using the three different precursors; TEOS, TMOS and Na_2SiO_3 is depicted schematically in Fig. 1. In order to compare the physical properties of silica aerogels prepared by using different precursors, the molar ratio of precursor, solvent and water kept constant at 1:5:7 respectively. Silica alcogels were prepared by hydrolysis and polycondensation of tetramethoxysilane diluted in methanol (MeOH), in the presence of ammonium hydroxide (NH_4OH) as a catalyst. Single step TMOS based gels were made from TMOS, CH_3OH and NH_4OH (Water) in the molar ratio of 1:5:7 respectively. The sol was transferred to Teflon moulds and kept at an ambient temperature of 23–30 °C. The gelation took place within 10 min.

Similarly, single step TEOS based gels were made from TEOS, CH_3OH and $C_2H_2O_4$ (Water) in the molar ratio of 1:5:7 respectively. But, the gelation time for TEOS based gel is 3.2 days.

For the preparation of sodium silicate based hydrogels, water–glass (Na_2SiO_3, s-d Fine chemicals, India, $SiO_2{:}Na_2O = 3.3$) solution was passed through an ion-exchanger, (Amberlite IR-120)to replace the Na^+ ions by H^+. The extent of ion exchange is known from the pH of the solution. The ion exchange is essential because Na^+ ions, poorly soluble in alcohol and trapped in the silica gel network tend to decrease the optical transmission of the dried gels. The collected silicic acid had a pH of ~2.3. The aquagels (thickness 3–8 mm and 3 cm diameter) were prepared by adding 1 M NH_4OH to the ion exchanged silicic acid while stirring. Gelation took place within 2 h at 50 °C.

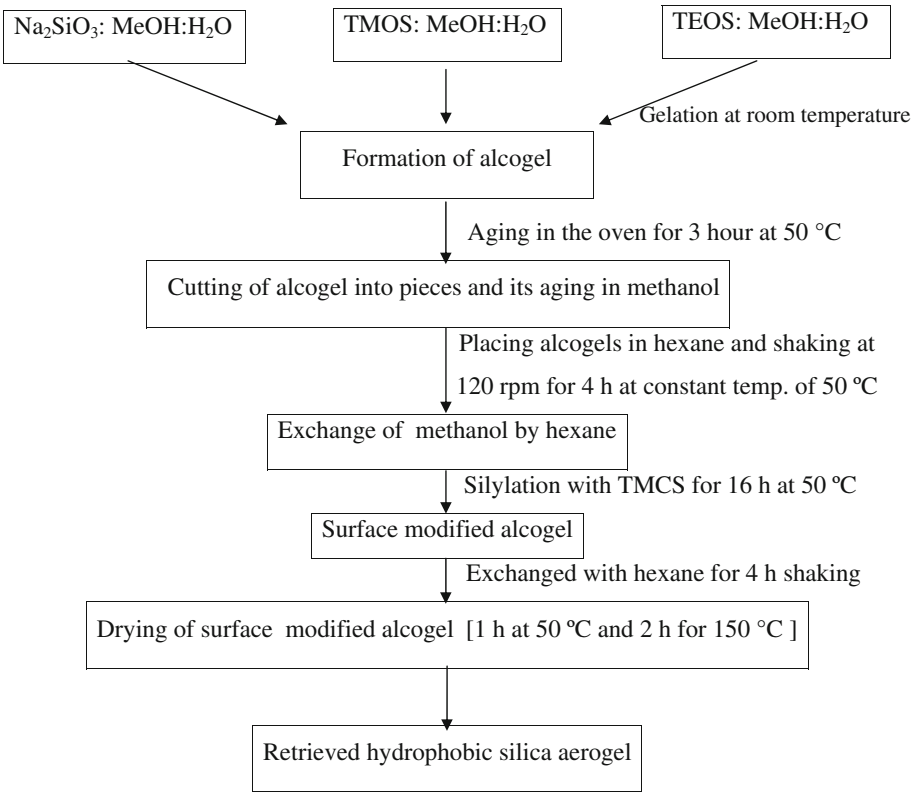

Fig. 1 Schematic of preparation of hydrophobic silica aerogels by using various precursors

After gelation, the gel was aged for 3 h at 50 °C to strengthen the gel network. After aging of the alcogels, they were cut into small cubic pieces which were then kept in methanol solvent for 10 min. The methanol was decanted out and hexane was added. The methanol in the wet silica gel was exchanged with hexane at 50 °C. The system was shaked at 120 rpm for 4 h in a shaker (Remi instruments, Mumbai, India). The surface modification was performed by immersing the gels in 5 % trimethylchlorosilane (TMCS) in n-hexane for 16 h at 50 °C. The unreacted TMCS was exchanged with the solvent (Hexane) by keeping again in the shaker for 4 h at 50 °C with 120 rpm speed. Finally, the alcogel pieces along with a little solvent were kept in the bottle. The bottle was covered with aluminum foil with 8–12 small pin holes to allow the evaporation of the solvent. Such bottles were kept in the oven at 50 °C for 1 h and at 150 °C for 2 h. The resulting aerogels were cooled to room temperature. The total processing period for one experiment is less than 2 days (40 h).

2.3 Methods of characterization

The bulk density, % of volume shrinkage, % of porosity and pore volume of the as prepared silica aerogels were measured using following formulae

$$\% \text{ of volume shrinkage} = \left(1 - \frac{V_a}{V_g}\right) \times 100 \quad (6)$$

$$\% \text{ of porosity} = \left(1 - \frac{\rho_b}{\rho_s}\right) \times 100 \quad (7)$$

$$\text{Pore volume} = \left(\frac{1}{\rho_b} - \frac{1}{\rho_s}\right) \quad (8)$$

where, V_a and V_g are the volume of the aerogel and alcogel respectively, ρ_s is the skeletal density ($\sim$1.9 mg cm^{-3}) and ρ_b is the bulk density.

Here, the density measurements of granules were conducted on the basis of weight of granules per unit volume in cc. The weights of aerogels were measured using Dhona microbalance (Model Dhona 100 DS) having a least count of 0.01 mg.

The thermal conductivity, K, of the aerogel was measured using thermal conductivity meter (C-T meter from Teleph Company, France accuracy 10^{-3} W/mK) with a thermal ring probe. The probe is sandwiched in between two identical aerogels under measurement.

The contact angle of the aerogels with water was measured using contact angle meter (Rame-Hart, Model 500 F-1, USA).

The Fourier Transform Infrared spectroscopic (FTIR) studies were carried out using Perkin Elmer (Model no. 760) IR spectrophotometer in the range 400–4000 cm^{-1}.

The surface morphology of the aerogel samples were studied using Scanning Electron Microscope (SEM), Model No. AIS2100 SEM, M/s Seron Technology, South Korea. For SEM analysis, aerogel samples were skillfully cut into $3 \times 3 \times 2$ mm^3 and were coated with gold in order to prevent electric charge during the SEM observation.

The specific surface areas were measured using a multi-point Brunauer, Emmett and Teller (BET) surface analyzer (Quantachrome instruments v10.0). The samples were degassed at around 200 °C for 2 h to remove the moisture. Liquid nitrogen (bath temperature 77.05 K) was used to measure the surface area. Pore parameters of silica aerogel samples were calculated using Brunauer, Emmett and Teller (BET) analytical method.

The thermal stability of the aerogels in terms of retention of hydrophobicity with temperature was estimated from thermo gravimetric and differential thermal analysis (TGA-DTA, SDT, 2960TA, USA).

3 Results and discussion

3.1 Density

From the present studies, it has been found that the precursors: TEOS,TMOS and Na_2SiO_3 strongly affect the physical properties like bulk density, percentage of porosity, surface area, contact angle, thermal conductivity and SEM of silica aerogels. Table 1 shows the effect of various precursors on some physical properties of silica aerogels. From Fig. 2a–c), it is clear that the aerogels produced using TMOS as the precursor, are more transparent than the aerogels prepared by TEOS and Na_2SiO_3 precursors. The higher density (34 g cm^{-3}) of TEOS based aerogel is the result of higher volume shrinkage due to weaker network composed of smaller silica particles linked together via longer chains. While, the Na_2SiO_3 based aerogels posses lowest density (23.3 g cm^{-3}) as compared to TEOS and TMOS aerogels.

The probability of fracture during drying is determined by the mechanical strength of the gel, permeability of the wet gel and the capillary pressure during drying. However, the mechanical strength, permeability of the Na_2SiO_3 based wet gel is higher than TEOS and TMOS based gels. Also, the pore size of TEOS based aerogel (2.90 nm) is very low as compared to Na_2SiO_3 (10.56 nm) and TMOS (11.80 nm) aerogels. Hence, the capillary pressure in case of TEOS is much higher than Na_2SiO_3 and TMOS based aerogels. This extremely high negative pressure pulls the wet TEOS gel inward during drying and therefore, the TEOS based gel shrinks more. Hence, the density of TEOS based aerogels is higher than that of TMOS and Na_2SiO_3. But due to high mechanical strength, high shear modulus and large pore size of Na_2SiO_3 gel, it has low density.

Figure 3a shows SEM picture of TEOS silica aerogel.

From Fig. 3a–c, it is clear that TEOS based silica aerogel contains large silica particles and small pores as compared to Na_2SiO_3 and TMOS aerogel. The smaller pore sizes lead to the decrease of the gel permeability to the fluid flow rate and hence resulted in cracked, dense TEOS aerogel. Scherer and Swaitek [20] concluded that the permeability of silica gels is strongly dependent on microstructure.

It is well known that the drying of a wet gel without surface modification causes its irreversible shrinkage due to the continuous condensation of end –OH groups leading to a dense aerogel. This is because capillary pressure exerted by pore fluid evaporation causes irreversible shrinkage in the silica aerogels. The capillary collapse in the wet gel can be prevented by replacing hydrophilic –OH groups on the surface of gel backbone with non-reactive Si–CH_3 species by means of surface chemical modification with silane coupling agents such as TMCS. The capillary pressure generated during drying is given by Laplace equation [21].

$$P = -2\frac{\gamma_{LV}\cos\theta}{r_p - \delta_t} \tag{9}$$

where γ_{LV} is the liquid–vapour surface tension, θ is the contact angle of the liquid with a pore wall, r_p is the pore radius and δ_t is the thickness of a surface adsorbed liquid layer. The negative sign is due to the negative radius of

Table 1 Effect of various precursors on some physical properties of silica aerogels

Precursor	Optimized molar ratio of Precursor:solvent:water	Gelation time (Tg)	Bulk density, (ρ_b) (Kg m^{-3})	Surface area (m^2 g m^{-1})	Average pore size (nm)	Thermal conductivity, (λ) (W m^{-1} K^{-1})	Contact angle,(θ) (°)
TEOS	TEOS:MeOH:H_2O 1:5:7	3.2 days	34	620	2.90	0.168	145
TMOS	TMOS:MeOH:H_2O 1:5:7	10 min	24.6	764	11.80	0.079	149
Na_2SiO_3	Na_2SiO_3:MeOH:H_2O 1:5:7	3 h	23.3	868	10.56	0.065	130

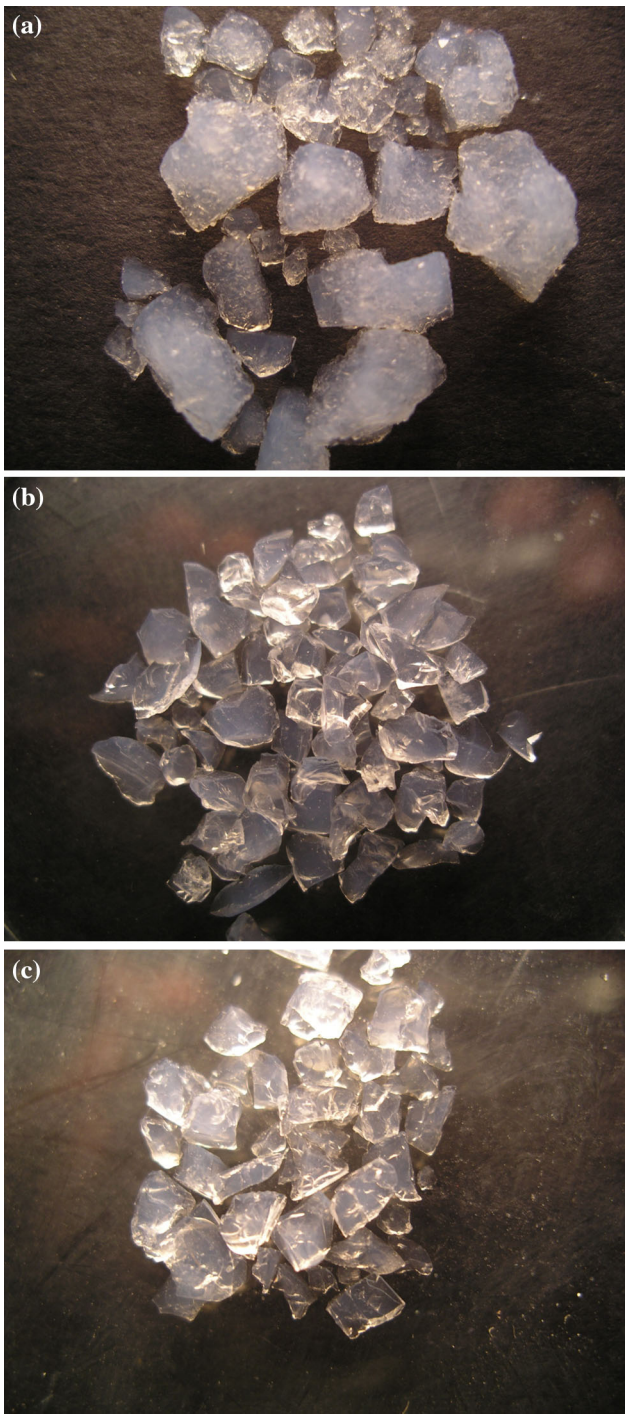

Fig. 2 **a** TEOS based silica aerogel, **b** TMOS based silica aerogel, **c** Na_2SiO_3 based silica aerogel

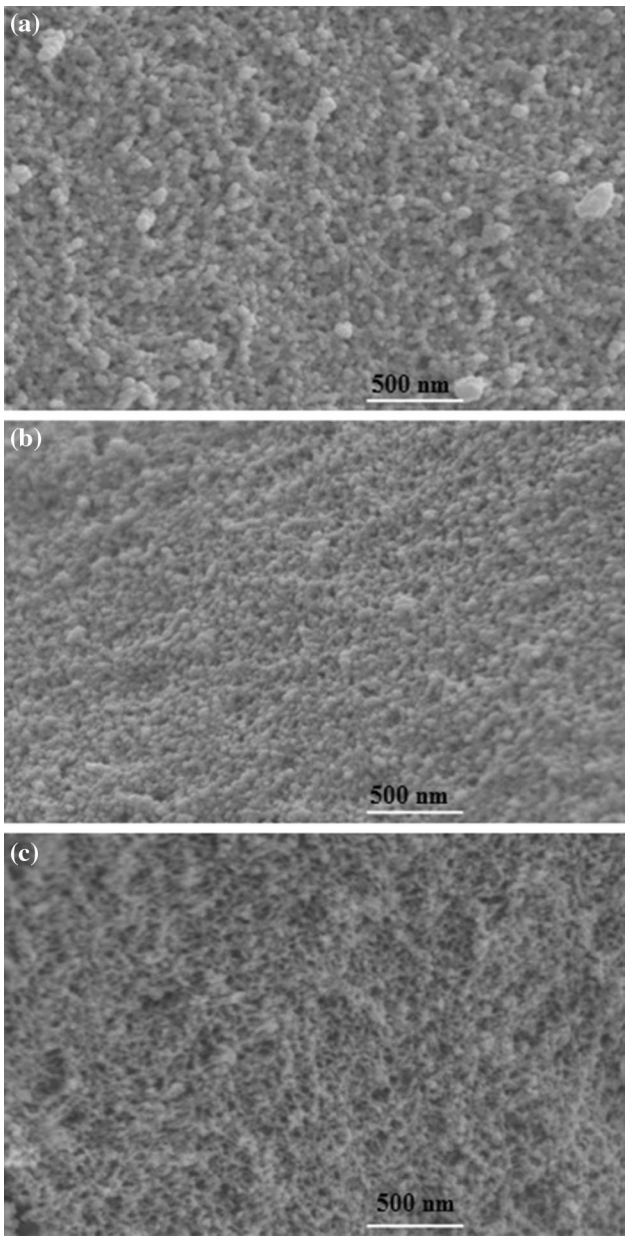

Fig. 3 **a** SEM image for TEOS based silica aerogels, **b** SEM image for TMOS based silica aerogels, **c** SEM image for Na_2SiO_3 based silica aerogels

curvature of the meniscus at the liquid–vapour interface. The TMCS minimizes the shrinkage of the gel through the reduction in surface tension of the solvent and contact angle between the solvent and the surface of silica network [22]. Due to high shear modulus, Na_2SiO_3 gel resist the capillary pressure during drying, so that the network of Si–OH stops contracting (i.e. CPD is reached). Here, CPD means Criticl Point Drying. At this stage, the gel network is chemically inert (Si–CH_3) groups are attached to the silica clusters due to the surface modification by TMCS), so that the shrunk gel completely springs back to its original volume. Therefore, the low density, large pore, semi-transparent and hydrophobic aerogels are obtained in the case of Na_2SiO_3. The attachment of Si–CH_3 groups to the

outer surface of cluster can be shown by following chemical reactions:

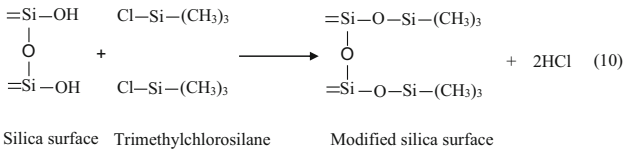

(10)

Another factor that affects the drying of gels is compressive stress. During the drying process, the evaporation of liquid from the gel creates a capillary tension (P) in the liquid. This tension is balanced by the compressive stresses on the solid network, causing shrinkage of the dried gel. The stresses during the drying depend on the interfacial energies (surface tension of pore liquid), the bulk modulus of the network and the pressure gradient in the liquid. According to Darcy's law, the liquid flow (J) through the gel is given by

$$J = (D/\eta_L)\nabla P \tag{11}$$

where D is the permeability of the gel, ∇P is the pressure gradient, and η_L is the viscosity of the liquid. During liquid evaporation, the pressure (P) in the liquid phase of the gel is related to the volumetric strain rate of the gel (ε) by

$$(D/\eta_L)\nabla^2 P = -\dot{\varepsilon} \tag{12}$$

The resulting stress in the solid phase of a gel plate of thickness L is given by

$$\sigma_X \approx C_N(L\eta_L \dot{V}_E/3D), \tag{13}$$

where $C_N \equiv (1 - 2\ N)(1 - N)$, N is Poisson's ratio, and is the liquid evaporation rate. Equation (13) indicates that the stress is proportional to the thickness of the gel plate and the liquid evaporation rate. Due to high permeability of the as well as Na_2SiO_3 gel, the compressive stress is small during the drying, causing the low shrinkage in TMOS and Na_2SiO_3 aerogel [20]. On the other hand, TEOS based gel has low permeability, so compressive stress during drying is high which leads to high shrinkage and in turns high density aerogels.

3.2 Micromorphology

Figure 3a–c shows the SEM photograph of different silica aerogel samples. The TMOS and Na_2SiO_3 aerogels (Figs. 3b, c) show almost all particles are spherical in shape while both particle and pores are smaller in size. On the other hand, it is clearly seen from Fig. 3a that TEOS aerogel shows larger silica particles and pores as compared to both TMOS and Na_2SiO_3 aerogels. From Fig. 3a, it is clearly seen that smaller size pores seem to look more in number compared to larger size pores. This leads to a wide Pore Size Distribution (PSD) with a shift towards smaller pore radii for the TEOS based aerogels. However, cracks are observed in TEOS based aerogels which is due to the low gel permeability to the fluid flow rate.

Scheidegger [23] gave detailed analysis of various stresses that develop during drying leading to cracks in the aerogels. He concluded that the large part of the stress results from syneresis (ε_S). Moreover, the permeability (D) value depends on the pore size (r) according to Carman-Kozeny equation [24]

$$\rho_b \alpha (1 - \rho_b) r^2 \tag{14}$$

where ρ_b is the density of the gel network. For a fixed ρ_b, lower r values decrease the permeability leading to cracks in the aerogels. Therefore, in order to obtain low density aerogels, larger D values are needed. In order to increased 'D' values, as of now Na_2SiO_3 precursor should be used for commercial production of low density and large surface area silica aerogels.

Figure 2a–c show photographs of the silica aerogels obtained using various precursors: (a) TEOS, (b) TMOS and (c) Na_2SiO_3.

3.3 Pore size distribution

It is clearly seen from Table 1 that the Na_2SiO_3 based aerogel sample has the biggest specific surface area while that of the TMOS based aerogel sample is smaller and the TEOS based aerogel sample is the smallest. Figure 4 clearly present the nitrogen adsorbed quantities and pore size distributions of the different samples. In Fig. 4, the adsorption–desorption isotherms of TEOS, TMOS and Na_2SiO_3 aerogels are of the typical type IV, belonging to mesoporous materials and the hysteresis loops of the type H_3 indicating the probable presence of slit-like interparticle pores [25, 26]. Furthermore, Fig. 5 shows that the most

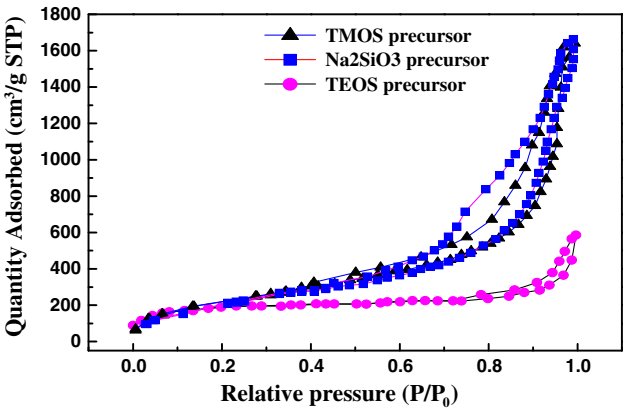

Fig. 4 Adsorption–desorption isotherms for TMOS, TEOS and Na_2SiO_3 based silica aerogels

probable pore diameter of the TMOS aerogel sample and Na_2SiO_3 aerogel sample and TEOS sample are 11.80, 10.56 and 2.90 nm, respectively. The TEOS based aerogel was highly dense with less surface modified gels and the compliant structure, and can freely shrink in response to solvent removal. The enormous capillary pressure attained at the final stage of the drying due to tiny pores causes a further compacting structure and leads to nanoporous structure of (2.90 nm) pore size distribution, whereas in the case of Na_2SiO_3 based aerogel, due to the absence of OH end groups condensation in the gels, there is a remarkable change in the structure due to inhibition of shrinkage, resulting in nanoporous structure, high pore volume with low dense aerogels with uniform pore size distribution of 10.56 nm.

It has been found that TMOS and Na_2SiO_3 based aerogels show high surface areas of 764 and 868 $m^2\ g^{-1}$, respectively. While, TEOS based aerogel possesses low (620 $m^2\ g^{-1}$) surface area compared to the TMOS and Na_2SiO_3 based aerogels. This is due to the fact that both the TMOS and Na_2SiO_3 based aerogels consist of smaller size SiO_2particles of the network whereas TEOS based aerogels consists of larger size SiO_2particles of the network as explained earlier.

During synthesizing SiO_2 aerogels, modification solvent plays an important role in determining the final microstructure. In our present studies, hexane is selected for surface modification of SiO_2 aerogel using TEOS, TMOS and Na_2SiO_3 as precursor before ambient pressure dying. The TEOS based silica aerogel formed some aggregates of spheres while the TMOS and Na_2SiO_3 based silica aerogel had porous structure with high porosity

TMOS based aerogels are more transparent than the TEOS based aerogels because the particle and pore sizes are small in the TMOS based aerogels compared to the TEOS based aerogels. This is due to the fact that the chain length and branching of the TMOS molecules is less than the TEOS molecules leading to faster hydrolysis and condensation processes in the former aerogels. Hence, the TMOS based aerogels have more optical transmission than the TEOS based aerogels.

3.4 Thermal conductivity

Generally, the thermal energy passing through an insulating material occurs by three mechanisms; solid conductivity, gaseous conductivity and radiative (infrared) transmission. The sum of these three components gives the total thermal conductivity of a material. Solid conductivity is an intrinsic property of a specific material. For dense silica, solid conductivity is relatively high (5 W/mK). However, silica aerogels possess a very small ($\sim$1–10 %) fraction of solid silica. Additionally, the solid that is present consists of very small particles linked in a three-dimensional network with many ''dead-ends''. Therefore, the thermal transport through the solid portion of silica aerogel occurs through a very tortuous path and is not particularly effective. The space, which is not occupied by solid in an aerogel, is normally filled with air. These air molecules can also transport thermal energy through the aerogel. The pores of silica aerogel are in the nano range (the pre sizes are smaller than the mean free path of air molecules). Therefore, the air molecules get trapped in the pores of the aerogel and therefore the convective heat transfer through the aerogel is also reduced. The final mode of thermal transport through silica aerogels is due to the radiation which has negligible effect under ambient conditions. Table 1 shows the thermal conductivity values for the aerogel obtained with different precursors. The thermal conductivity of the TEOS based aerogels measured at room temperature has been found to be 0.168 W/mK whereas the measured thermal conductivity values for TMOS and Na_2SiO_3 based aerogels have been found to be 0.079 and 0.065 W/mK, respectively. The thermal conductivity as a function of the bulk density of the aerogel. The bulk density of sodium silicate based aerogel is lower as compared to TMOS and TEOS based silica aerogels. Also, pore size of Na_2SiO_3 aerogels is relatively higher than TEOS based aerogels. Therefore, the convective heat transfer through Na_2SiO_3 aerogels is relatively low as compared to TEOS based aerogels. As the bulk density of the aerogel decreases, the silica network becomes more porous leading there by less solid content. Therefore, the thermal conductivity of aerogel is less. Hence, the thermal conductivity of Na_2SiO_3 based aerogels is lower than the TMOS and TEOS based silica aerogels. From the SEM micrographs, it is clear that silica network is dense in TEOS and TMOS based aerogels than that of Na_2SiO_3 based aerogels. Therefore, the thermal conductivity of Na_2SiO_3 based aerogels is expected to be less than that of TMOS and TEOS based aerogels.

3.5 FTIR analysis and hydrophobicity

For, TMOS based aerogel, it has been observed form Fig. 6 that the C–H absorption peaks at 1440 and 2900 cm^{-1} are strong while O–H peaks at around 1600 and 3450 cm^{-1} are weak, indicating hydrophobic nature of aerogel [27].

While in case of TEOS and Na_2SiO_3 based aerogels, C–H absorption peaks at 1450 and 2930 cm^{-1} are weak as compared to TMOS aerogel. This fact is reflected in contact angle measurement. The TEOS, TMOS based aerogels are more hydrophobic as compared to Na_2SiO_3 based aerogels.

Figure 7a–c are the photograph of the contact angle test, and the contact angles of each sample with different

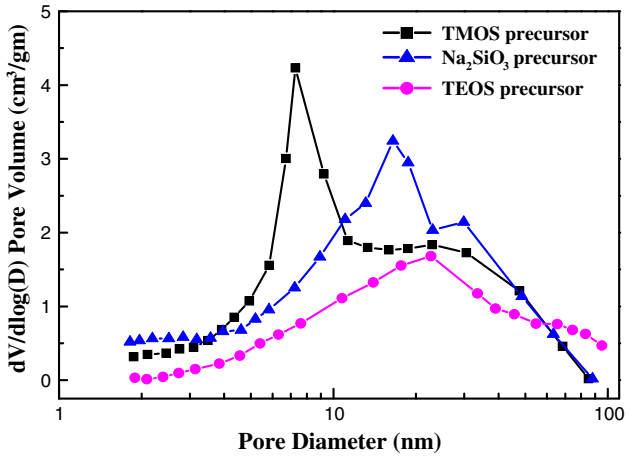

Fig. 5 Pore size distribution for the TMOS, TEOS and Na_2SiO_3 based silica aerogels

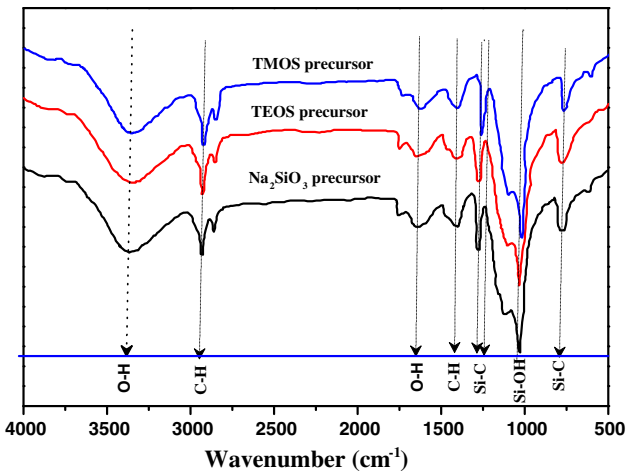

Fig. 6 FTIR spectra of TEOS, TMOS and Na_2SiO_3 based silica aerogels

precursor are listed in Table 1. The hydrophobicity of aerogel is mainly determined by surface chemical groups which have been discussed above using FTIR spectra. It is obviously that both the TMOS based and TEOS based aerogels have large angle of contact 149° and 145° respectively, which are much higher than that of the Na_2SiO_3 based aerogel (130^0). This is due to the fact that the TMOS and TEOS are highly reactive than the Na_2SiO_3 precursor. Tetramethoxysilane (TMOS) undergoes a more rapid hydrolysis than tetraethoxysilane (TEOS).

The rate of hydrolysis and condensation of TEOS is higher than that of the Na_2SiO_3 but lower than the TMOS. Any branching of alkoxy groups or lengthening of the chain slows the hydrolysis rate of the alkoxysilanes. The reaction rate decreases in the following order: Si(OMe)4 > Si(OEt)4 > Si(O*n*Pr)4 > Si(O*i*Pr)4 [28]. Therefore, the TMOS as well as the TEOS precursors give rise to more silanol (Si–OH) concentration than the Na_2SiO_3 precursor. Hence, during the surface chemical modification, more number of the O–Si–$(CH_3)_3$ hydrolytically stable groups get attached to the Si–OH groups through oxygen bonds as shown in reaction (10). Due to more silylation, aerogel surface pores are covered with more Si–CH_3 groups and does not allow water to enter into the pores so that the aerogels have better withstanding power of hydrophobic coverage against water. While in case of Na_2SiO_3 based aerogel, due to less silylation, the aerogel surface pores are covered with less Si–CH_3 groups and hence, some water molecule can enter into pores of aerogel.

It is observed that as compared to TEOS based gels, Na_2SiO_3 and TMOS based gels spring back to almost its original volume of the wet gel when the evaporation of hexane is completed. This might be due to the fact that in the case of Na_2SiO_3 and TMOS based gels the more number of surface methyl groups prevents the pore collapse during solvent evaporation (spring-back effect) under ambient conditions as compared to TEOS based gels. The TMOS and the Na_2SiO_3 (silicic acid) based silica gels have less chain length and less branching compared to the TEOS based silica gels and hence resulting in more silylation in the case of the aerogels based on the former precursors. Therefore, this leads to more spring back effect in the case of TMOS and Na_2SiO_3 based aerogels.

3.6 TGA DTA

The thermal stability of the aerogels in terms of retention of hydrophobicity was estimated from the thermogravimetric and differential thermal analysis (TG–DTA) as well as heating the aerogels at different temperatures in the furnace and putting the cooled samples over the water surface. The retention of the hydrophobicity (water repelling property) was judged from the absorption of water by the aerogels. Figure 8a–c shows the TG–DTA analysis of the TEOS, TMOS and Na_2SiO_3 based aerogels in the oxygen atmosphere up to 700 °C. The TGA and DTA studies in the oxygen atmosphere revealed that all the chemically modified gels are thermally stable up to a temperature of 415 °C and above the 415 °C, the weight of all the aerogel samples decrease due to the oxidation of the methyl groups leaving the silica network. This fact can be clearly seen as there is a sharp exothermic peak in the DTA curve when the temperature raised above 400 °C. The sharpness of the peak in the case of TMOS and TEOS is high as compared to Na_2SiO_3 because more number of methyl groups are attached to the TMOS and TEOS than

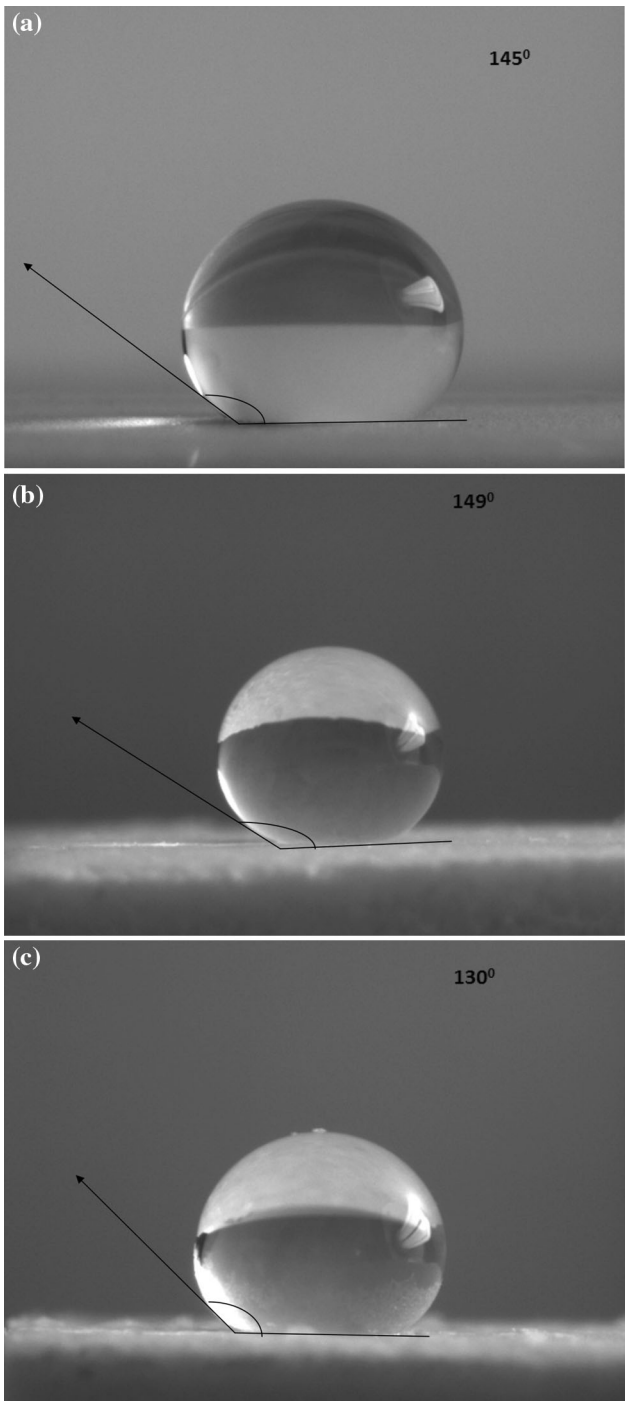

Fig. 7 Water droplet on the **a** TEOS based silica aerogel (145°), **b** TMOS based silica aerogel (149°), **c** Na_2SiO_3 based silica aerogel (130°)

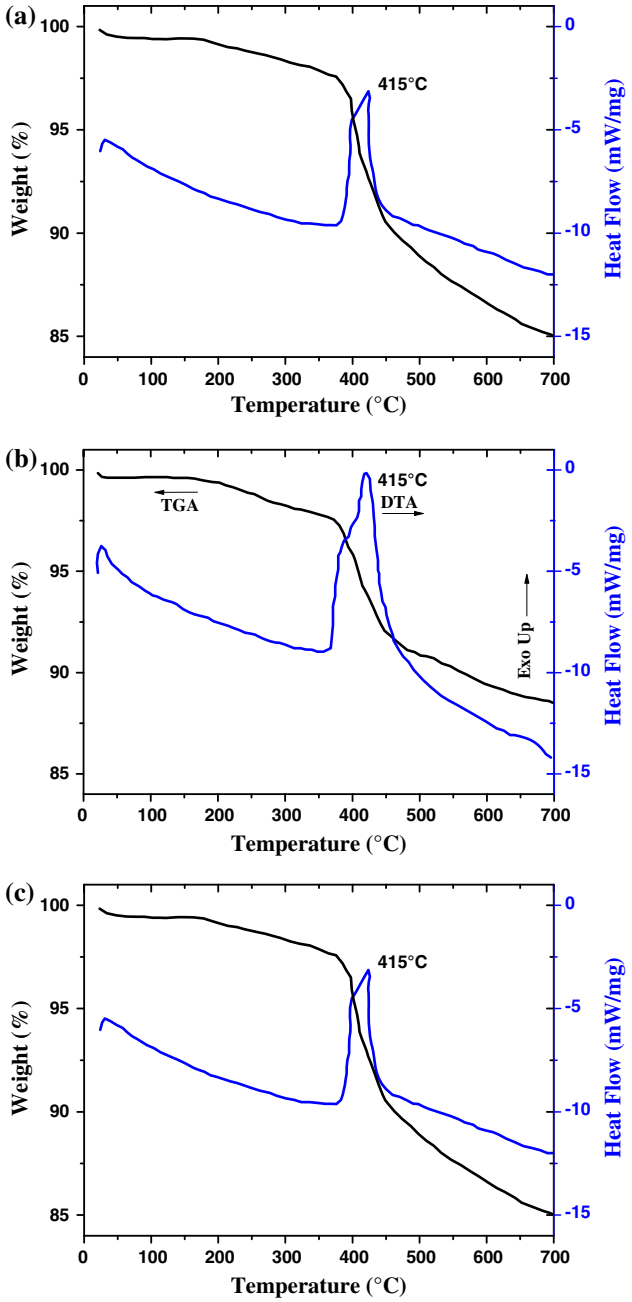

Fig. 8 **a** TG-DSC graph for TMOS based silica aerogels, **b** TG-DSC graph for TEOS based silica aerogels, **c** TG-DSC graph for Na_2SiO_3 based silica aerogels

that of Na_2SiO_3. It can be also seen in the TGA curves as the weight loss in Na_2SiO_3 aerogel is less than TMOS and TEOS aerogels because of less surface modification in TMOS, TEOS aerogels than Na_2SiO_3 aerogel so less number of methyl groups that undergo oxidation than the TMOS, TEOS aerogels.

4 Conclusions

Silica aerogels of different physical properties have been obtained using three different precursors namely TMOS, TEOS and Na_2SiO_3. The differences among the physical properties of silica aerogels prepared by the three different precursors are explored in detail. The microstructures of the aerogels were determined by the sol–gel reaction. It has been found that the surface area of the TMOS, TEOS and

Na_2SiO_3 aerogels are ~764, 620 and 868 $m^2 g^{-1}$, respectively. Although all of the three precursors could obtain mesoporous structures, the Na_2SiO_3 based aerogel had better uniform pore size distribution with the most probable pore diameter of 7 nm and average pore size of 12 nm. Through surface modification, the organic groups ($Si\text{-}CH_3$) were attached either on the inside or on the surface of the skeletons which assisted to resist the lateral compressive stresses during the APD and provided the chemical basis for the hydrophobicity of the aerogels. Among the three aerogels, the TMOS based aerogel method had the lowest intensity of: Si–OH groups which suggested the excellent hydrophobicity with the largest contact angle of 149°.

Acknowledgments The corresponding author is highly thankful to the UGC, New Delhi, India, for the funding this work under University Grant Commission-Basic Science Research (UGC-BSR) Faculty Fellowship No. F.18-1/2011 (BSR). One of the authors, Abhijit A. Pisal is highly grateful to the UGC, New Delhi, for the Stipendiary Candidateship under UGC-BSR-Faculty Fellowship.

References

1. C.A.M. Mulder et al., in *Aerogels*, ed. by J. Fricke (Springer, Berlin, 1986), p. 68
2. T. Burger, J. Fricke, Aerogels: production, modification and applications. Ber. Bunsenges. **102**, 1523–1528 (1998)
3. J. Gross, J. Fricke, Ultrasonic velocity measurements in silica, carbon and organic aerogels. J. Non Cryst. Solids **145**, 217–222 (1992)
4. E. Cuce, P.M. Cuce, C.J. Wood, S.B. Riffat, Toward aerogel based thermal superinsulation in buildings: a comprehensive review. Renew. Sustain. Energy Rev. **34**, 273–299 (2014)
5. M.M. Koebel, A. Rigacci, P. Achard, Aerogel-based thermal superinsulation: an overview. J. Sol-Gel. Sci. Technol. **63**, 315–339 (2012)
6. J.G. Reynolds, P.R. Coronado, L.W. Hrubesh, Hydrophobic aerogels for oil-spill cleanup—synthesis and characterization. J. Non Cryst. Solids **292**(1–3), 127–137 (2001)
7. I. Smirnova, S. Suttiruengwong, W. Arlt, Feasibility study of hydrophilic and hydrophobic silica aerogels as drug delivery systems. J. Non Cryst. Solids **350**(2004), 54–60 (2004)
8. G.M. Pajonk, S.J. Teichner, J. Fricke (eds.), *Aerogels* (Springer, NewYork, 1986), pp. 193–199
9. G.M. Pajonk, Aerogel catalysts. Appl. Catal. **72**, 217–266 (1991)
10. J. Fricke, A. Emmerling, Aerogels—recent progress in production techniques and novel applications. J. Sol-Gel. Sci. Technol. **13**(1–3), 299–303 (1999)
11. U.K.H. Bangi, A.V. Rao, A.P. Rao, A new route for preparation of sodium silicate-based hydrophobic silica aerogels via ambient-pressure drying. Sci. Technol. Adv. Mater. **9**, 035006 (2008)
12. L.-J. Wang, S.-Y. Zhao, M. Yang, Structural characteristics and thermal conductivity of ambient pressure dried silica aerogels with one-step solvent exchange/surface modification. Mater. Chem. Phys. **113**, 485–490 (2009)
13. Hajar Maleki, Luisa Duraes, Antonio Portugal, Development of mechanically strong ambient pressure dried silica aerogels with optimized properties. J. Phys. Chem. C **119**, 7689–7703 (2015)
14. D.B. Mahadik, A.V. Rao, P.B. Wagh, S.C. Gupta, Synthesis of transparent and hydrophobic TMOS based silica aerogels. AIP Conf. Proc. **1536**, 553 (2013)
15. Wim J. Malfait, Shanyu Zhao, Rene Verel, Subramaniam Iswar, Daniel Rentsch, Resul Fener, Yucheng Zhang, Barbara Milow, Matthias M. Koebel, Surface chemistry of hydrophobic silica aerogels. Chem. Mater. **27**(19), 6737–6745 (2015)
16. S. Hea, Z. Lia, X. Shia, H. Yanga, L. Gonga, X. Cheng, Rapid synthesis of sodium silicate based hydrophobic silica aerogel granules with large surface area. Adv. Powder Technol. **26**(2), 537–541 (2015)
17. P.B. Wagh, R. Begag, G.M. Pajonk, A.V. Rao, D. Haranath, Comparison of some physical properties of silica aerogel monoliths synthesized by different precursors. Mater. Chem. Phys. **57**, 214–218 (1999)
18. D.B. Mahadik, A.V. Rao, The ambient pressure dried TEOS based silica aerogel granules. J. Porous Mater. **19**(1), 87–94 (2012)
19. P.B. Sarawade, J.-K. Kim, A. Hilonga, D.V. Quang, H.T. Kim, Synthesis of hydrophilic and hydrophobic xerogels with superior properties using sodium silicate. Microporous Mesoporous Mater. **139**, 138–147 (2011)
20. G.W. Scherer, R.M. Swiatek, Measurement of permeability: II. Silica gel. J. Non Cryst. Solids **113**(2–3), 119–129 (1990)
21. E. Nilsen, M.-A. Einarsrud, G.W. Scherer, J. Non Cryst. Solids **221**, 135 (1997)
22. D.M. Smith, G.W. Scherer, J.M. Anderson, J. Non Cryst Solids **188**, 191 (1995)
23. A.E. Scheidegger, *The Physics of Flow Through Porous Media*, 3rd edn. (University of Torento Press, Torento, 1974)
24. P.M. Adler, Transport processes in fractals. VI. Stokes flow through Sierpinski carpets. Phys. Fluids **29**, 15 (1986)
25. F. Rojas, I. Kornhauser, C. Felipe, J.M. Esparza, S. Cordero, A. Dom-ínguez, J.L. Riccardo, PCCP Phys. Chem. Chem. Phys. **22**, 2346–2355 (2002)
26. S.A. Lermontov, A.N. Malkova, L.L. Yurkova, E.A. Straumal, N.N. Gubanova, A.Y. Baranchikov, V.K. Ivanov, Mater. Lett. **116**, 116–119 (2014)
27. D.B. Mahadik, Y.K. Lee, N.K. Chavan, S.A. Mahadik, H.-H. Park, Monolithic and shrinkage-free hydrophobic silica aerogels via new rapid supercritical extraction process. J. Supercrit. Fluids **107**, 84–91 (2016)
28. U. Schubert, N. Hüsing, *Synthesis of inorganic materials* (Wiley-VCH, Weinheim, 2005), pp. 92–221